Sensors & Actuators: B. Chemical 304 (2020) 127380

Contents lists available at ScienceDirect

Sensors and Actuators B: Chemical

journal homepage: www.elsevier.com/locate/snb

Ultrasensitive evaluation of Ribonuclease H activity using a DNAzyme-powered on-particle DNA walker

Wenjing Wang[1], Mingbo Shu[1], Axiu Nie, Heyou Han*

State Key Laboratory of Agricultural Microbiology, College of Science, Huazhong Agricultural University, Wuhan 430070, People's Republic of China

ARTICLE INFO

Keywords:
RNase H activity
DNA walker
DNAzymes
Signal amplification
RNase H inhibitor

ABSTRACT

The evaluation of Ribonuclease H (RNase H) activity is very important for anti-HIV drug development and the study of cellular processes, including DNA replication, DNA repair and transcription. However, the highly sensitive detection of RNase H activity with a simple strategy remains challenging. Here, a DNAzyme-powered on-particle DNA walker was proposed as a signal amplifier to evaluate the RNase H activity at levels as low as 0.00847 U mL^{-1}. Pre-caged enzyme strands and substrate strands of Mn^{2+}-specific DNAzyme were modified at the interface of gold nanoparticles, forming the DNA walker probes. In the absence of RNase H, a minimum fluorescent signal was observed due to excellent ability of gold nanoparticles to quench the fluorophore that labeled the substrate strand. In the presence of RNase H, the DNA/RNA hybrid complex was hydrolyzed to release single stranded DNA, which was able to hybridize to the locker strand that caged the enzyme strand. Following the addition of Mn^{2+}, the active forms of DNAzymes were cleaved at the RNA site of substrate strands, releasing enhanced fluorescent molecules. Finally, the walker strands traveled over the AuNPs like a machine to amplify the signal, thus indirectly measuring the activity of RNase H. This approach proved to be an ultrasensitive and simple method for the evaluation of RNase H activity in cell extracts and has also been successfully used to evaluate the effects of inhibitors.

1. Introduction

Ribonuclease H (RNase H) is a processive endonuclease that specifically hydrolyzes the RNA strand in RNA/DNA hybrids [1,2]; the hydrolysis occurs from the 3′ end of RNA, yielding digestion products with a 3′-hydroxyl and 5′-phosphate at the termini [3,4]. This enzyme is reported to play a vital role in the cellular processes of DNA replication, DNA repair and transcription [5–7]. More importantly, RNase H activity is essential for the replication of human immunodeficiency virus (HIV) [8]. Considering the drug resistance of the continuously emerging HIV variants to drugs that are currently used in the clinic, RNase H has become a new target and effective alternative for antivirus drug development [9–11]. Therefore, the development of simple and sensitive method to evaluate the activity of RNase H is urgently needed for related biological studies and new anti-HIV drug screens.

Previously developed methods for evaluating RNase H activity are gel electrophoresis [12], capillary electrophoresis [13] and acid-soluble release of the RNA fragment [14]. The inherent drawbacks include the requirement for radioisotope labeling, time-consuming and laborious procedure that hinder their further applications. These challenges have been addressed in the recent studies, a series of colorimetric [15] and fluorescence assays to evaluate of RNase H activity have been proposed. In particular, fluorescence strategies based on molecular beacons [16–18], intercalating reagents [19–22] and graphene oxide [23], among others, have attracted extensive attention due to the high sensitivity, ease of operation, and simplicity. Although these methods have provided superior detection performance compared with the traditional methods, the limit of detection and dynamic range must be further improved by coupling the methods with an effective signal amplification strategy.

Taking advantage of the high loading capability of nanoparticles and excellent mobility and processivity of DNA nanodevices, on-particle DNA walkers have recently been widely explored as powerful signal amplification tools for biosensing applications. Gold nanoparticles (AuNPs) are easy to synthesize and modify; they also possess interesting size and shape dependent plasmonic properties. Therefore, AuNPs are ideal carriers of immobilized DNA and are widely used to construct on-particle DNA walkers. Elaborately designed DNA sequences are attached to the AuNPs to form the walker probes. The presence of targets enables the "walker" to walk along the "track" on

* Corresponding author.
E-mail address: hyhan@mail.hzau.edu.cn (H. Han).
[1] Equal contribution.

https://doi.org/10.1016/j.snb.2019.127380
Received 10 June 2019; Received in revised form 1 November 2019; Accepted 4 November 2019
Available online 05 November 2019
0925-4005/

the surface, causing signal amplification to sensitively and selectively quantify analytes. This principle was initially used to detect protein and nucleic acid. Targets triggered the proximity of DNA-modified AuNPs and walker sequences, and the further addition of a nicking endonuclease powered the walker to walk along the whole nanoparticle, amplifying the fluorescent signal for in vitro detection [24]. A similar system was employed to release a payload [25] and discriminate single nucleotide variants [26] as well, showing great potential for cancer therapy and diagnosis. The on-particle DNA walker was further developed by replacing the nicking endonuclease with DNAzymes using metal ions as a cleavage cofactor [27]. Considering the good biocompatibility of AuNPs, this system has recently been utilized as a sensor for intracellular miRNAs [28].

In more detail, the energy required to power the on-particle DNA walker is typically derived from the following sources: protein enzymes, including endonucleases [29] and exonucleases [30], entropy [31] and RNA-cleaving DNAzymes [28]. Protein enzymes specifically recognize the cleavage site either in the middle of the track sequences (for endonucleases) or the end of the track sequences (for exonucleases) to activate and reuse the walker on the particle to amplify the biosensing signals. Although these enzymes have a high amplification efficiency, the low stability and high cost of protein enzymes limit their further applications. In contrast, entropy-driven on-particle DNA walkers avoid the involvement of protein enzymes and are based on the competitive hybridization between DNA strands; however, the design of strands is achieved through a time-consuming trial and error process. Compared with these aforementioned strategies using protein enzymes, RNA-cleaving DNAzymes-powered DNA walkers have additional benefits, such as their low cost and ease of design, thus, they have received extensive attention in amplified biosensing [27,32–36].

Here, we developed a DNAzyme-powered on-particle DNA walker for the ultrasensitive detection of RNase H activity. Thirteen nanometer gold nanoparticles (AuNPs) serving as nanocarriers were modified with substrate strands and caged enzyme strands of Mn^{2+}-specific DNAzymes. The enzyme strands were pre-hybridized with locking strands to inhibit binding with their corresponding substrate strands. The substrate strands were modified with fluorescent molecules that were quenched by AuNPs and produced a minimal fluorescent signal. In the presence of RNase H, the RNA sequences in DNA/RNA complexes were hydrolyzed, allowing the free DNA strands to hybridize with the locking strands via the toe-hold mediated strand displacement reaction. The de-caged enzyme strands at the interface of AuNPs bind to nearby substrate strands. Following the addition of Mn^{2+}, the active form of DNAzymes were cleaved at the RNA site of substrate strands releasing enhanced fluorescent molecules. Subsequently, the walker moved to the next substrate strand and repeated the cleavage process. Finally, the walker strands traveled the AuNPs like a machine to amplify the signal, thus indirectly measuring the activity of RNase H. This study is the first to report the use an on-particle DNA walker as signal amplification strategy to detect RNase H with significantly improved detection performance, and the excellent stability of AuNPs might facilitate their use in analyzing more complex samples, such as cell extracts.

2. Experimental section

2.1. Reagents and apparatus

All the DNA and RNA sequences used in this study are listed in Table S1. They were synthesized by Sangon Biotechnology Co. Ltd. (Shanghai, China) with HPLC purification for modified sequences and UltraPAGE purification for other sequences.

The 40% acrylamide mixed solution, 1, 2-bis(dimethylamino)-ethane (TEMED), ammonium persulfate (APS), diethylpyrocarbonate (DEPC)-treated water and DNA ladder were obtained from Sangon Biotechnology Co. Ltd. (Shanghai, China). Exonuclease I, Hind III and Dpn I were purchased from Thermo Fisher Scientific (Waltham, MA, USA). RNase H and mung bean nuclease were obtained from NEW England Biolabs (Beverly, MA, USA). Tris-(2-carboxyethyl) phosphine hydrochloride (TCEP) was purchased from Sigma-Aldrich (St. Louis, MO, USA). Tween-20, chloroauric acid ($HAuCl_4$) and trisodium citrate were provided by Sinopharm Chemistry Reagent Co. Ltd. (Shanghai, China). Ellipticine was provided by TargetMol Co. Ltd. (Shanghai, China). Tris-HCl buffer (25 mM, with 100 mM NaCl, pH = 7.4) was used in this study. All other chemicals were of analytical grade and were used as received without any further purification.

2.2. Polyacrylamide gel electrophoresis (PAGE) characterization

The feasibility of the designed DNA sequences was verified and characterized using PAGE. Ten microliters of each sample were loaded on 12%, 1 mm polyacrylamide gels. Electrophoresis was performed in 1 × TBE buffer at 120 V for 100 min. The gel was stained after separation and imaged with the fluorescence gel imaging system.

2.3. Preparation of DNAzyme-powered on-particle DNA walker probes

First, 13 nm AuNP carriers were synthesized as described in a previous report [34]. Briefly, 100 mL of a 1 mM $HAuCl_4$ solution was boiled to reflux in a three-neck flask; then, 10 mL of a 38.8 mM sodium citrate solution were added in one quick motion under vigorous stirring. The color changed from pale yellow to deep red. The solution was stirred for 15 min, removed from the hot plate, and stirred for another 15 min at room temperature. The mixture was cooled to room temperature, and then stored at 4 °C until further use. Subsequently, the substrate strands and caged enzyme strands were attached to 13 nm AuNPs as previously reported to prepare DNA walker probes [34]. Next, 0.3 μL of the 141 μM enzyme strand solution was mixed with 0.9 μL of the 141 μM locking strands, and 0.3 μL of 5 × PBS (100 mM NaH_2PO_4, 100 mM Na_2HPO_4, and 500 mM NaCl, pH = 7.4) in a PCR tube and heated to 90 °C for 5 min. After the solution was slowly cooled to room temperature over more than 2 h, 1.2 μL of 10 mM TCEP in acetate buffer (50 mM, pH 5.2) were added to activate the thiol groups for further use. Meanwhile, 6.1 μL of the 139 μM substrate strand solution and 1.2 μL of 100 mM TCEP in acetate buffer (50 mM, pH 5.2) were mixed in another PCR tube. Both tubes were incubated at room temperature for 1 h. Finally, the solutions in the two tubes were mixed and slowly added to 100 μL of pre-cooled AuNPs. After thorough vertexing, the mixture was incubated in a refrigerator at 4 °C for 16 h. The salt-aging method was employed to improve the loading efficiency of DNA strands. Specifically, 1.0 μL of NaCl (2.5 M) solution was added 4 times at intervals of 8 h. The mixture was purified by four centrifugation steps at 12,000 rpm for 30 min each to remove the excess DNA strands. The DNA walker probes were finally redispersed in Tris buffer and stored at 4 °C until further use.

2.4. Fluorescent assay of RNase H activity

We initially annealed the DNA/RNA complexes by mixing the DNA strand and RNA strand at an equivalent ratio of 1:1.2 in RNase H reaction buffer (RNase-free, 10 mM Tris, 50 mM NaCl, and 10 mM Mg^{2+}, pH = 7.9). The mixture was heated to 80 °C for 5 min, and slowly cooled to room temperature. Next, a 100 nM solution of the as-prepared DNA/RNA complexes was mixed with different concentrations of RNase H in a total volume of 5 μL and incubated at 37 °C for 60 min, followed by an incubation at 70 °C for 20 min to deactivate the enzyme activity. The aforementioned 5 μL solution was further mixed with 10 μL of 5 mM Mn^{2+} and 0.5 μL of AuNP probes. The mixture was then diluted to 100 μL with Tris-HCl buffer (25 mM Tris-HCl and, 100 mM NaCl, pH = 7.4) and incubated at 25 °C for 1 h. The fluorescence spectra were measured using a Shimadzu RF-5301PC fluorescence spectrophotometer (Shimadzu Corp., Tokyo, Japan). The fluorescence intensity was monitored by exciting the sample at 495 nm and measuring the

emission at 520 nm. The slit widths for both excitation and emission were set to 5 nm.

For control samples, we added water or EDTA instead of DNA/RNA complexes or Mn^{2+} respectively, and the other steps were the same as described above. For the specificity test, we replaced RNase H with blank buffer, Dpn I, Exo I, Hind III and mung bean nuclease in the aforementioned procedures, and the other procedures were the exactly the same. For the RNase H inhibitor screen assay, we initially incubated various concentrations of ellipticine with RNase H (5 U mL^{-1}) at 37 °C for 10 min, and then followed the same protocol as described above.

2.5. Evaluation of RNase H activity in cell lysates

The cell lysate was prepared using a previously reported protocol [35]. In order to prepare cell lysate, we cultured human cervical cancer cells (HeLa), human lung adenocarcinoma cells (A549), human liver cancer cells (HepG2) and breast cancer cells (4T1) in DMEM (Gibco, Grand Island, NY) supplemented with 10% fetal calf serum (Gibco, Grand Island, NY), penicillin (100 μg/mL) and streptomycin (100 μg/mL) in a 5% CO_2, incubator at 37 °C. Approximately 5×10^5 cells were collected and dispensed in a 1.5 mL Eppendorf tube in the exponential phase of growth, followed by two washes with ice-cold phosphate buffered saline (pH = 7.4) and resuspended in 500 μL of ice-cold cell lysis buffer (50 mM Tris-HCl, 150 mM NaCl, 0.1% SDS, 0.5% deoxycholic acid and protease inhibitor of 0.1 mM PMSF). The mixture was incubated on ice for 20 min and then centrifuged for 30 min (12,000 rpm at 4 °C). Finally, the cleared lysate was carefully transferred to a fresh tube without disturbing the pellet and stored at −20 °C until use. The cell lysates were employed as reaction media instead of water to test the feasibility of our proposed method to evaluate the RNase H activity in a real sample. Other procedures were the same as described above.

3. Results and discussion

3.1. Principle of the proposed biosensor

The principle of the DNAzyme-powered on-particle DNA walker designed to evaluate RNase H activity is illustrated in Scheme 1. A truncated form of 8–17 DNAzymes was employed to construct the sensing probe, and the sequences were adapted from previous report, which has successfully been used for the intracellular miRNA imaging [28]. Specifically, ployT spacers with lengths of 14 bases' and 42 bases' were added to the 5′ end of the substrate strand and enzyme strand, respectively, to increase the accessibility of the substrate strand on the AuNP by the free enzyme strand. Both strands were simultaneously anchored onto AuNPs via Au-S chemistry at the 5′ ends, at the optimized equivalent ratio of 20:1 substrate strand to enzyme strand, according to a previous study [28]. The 3′ end of the substrate strand was modified with carboxyfluorescein (FAM), which was quenched by the AuNPs. The enzyme strand was caged by a locking strand through the complementary hybridization of 22 bases; 6 of these bases were essential for the formation of the active DNAzyme, preventing substrate strand cleavage (Fig. S1).

Meanwhile, in the presence of RNase H, the RNA strand in DNA/RNA complex was specifically hydrolyzed. The DNA strand remaining after the hydrolysis de-caged the enzyme strands through hybridization with 7 bases of the locking strand via toe-hold mediated strand displacement. Free enzyme strands readily hybridized with the substrate strand, generalizing active DNAzymes. In the presence of Mn^{2+}, the substrate strand was cleaved at the single-ribonucleotide junction into two parts. Both parts detached from enzyme strand due to the significantly decreased melting temperatures; therefore, the fluorescence was recovered (Fig. S2), and the free enzyme strand traversed the nearby substrate strand again. Each movement of the enzyme strand resulted in the cleavage of the anchored substrate strands accompanied by the release of fluorescently labelled DNA strands from AuNPs, leading to an increase in the fluorescence that enable the quantification of RNase H activity.

3.2. Characterization of DNA walker probes

We first synthesized and characterized the DNA walker probes. As shown in Fig. 1A, the bare AuNPs showed excellent dispersity with an approximate mean size of 13 nm. After functionalization with substrate strands and caged enzyme strands, there was minimal change in the dispersity, indicating the modification had negligible effect on AuNPs (Fig. 1B). Bare AuNPs exhibited a maximum absorption peak at 520 nm (Fig. 1C, curve a), while DNA walker probes displayed a 4 nm red-shift of the maximum absorption peak (Fig. 1C, curve b). In addition, the dynamic light scattering (DLS) data (Fig. 1D) revealed an increase in the size of AuNPs from 14.3 nm to 19.1 nm, suggesting the successful attachment of DNA. Similarly, Zeta potential of AuNPs decreased significantly after the attachment of negatively charged DNA molecules. (Fig. S3) Mercaptoethonal (MCE) was employed to replace thiolated strands modified at the interface of AuNPs to quantify the number of DNA strands attached to each AuNP. According to the calibration curves and the fluorescence spectrum of the MCE-treated sample (Fig. S4), the number of substrate strands attached to each AuNP was 132 ± 18, and the number of caged enzyme strands was calculated to be 11 ± 2. Altogether, these data confirm the successful modification of AuNPs, and the DNA walker probes were prepared as expected for further use. We studied the stability by monitoring the fluorescent signal change along with time. We tested the freshly synthesized DNA walkers for three weeks (21 days). As shown in Fig. S5, there is minimum change in the fluorescent signal for all the tested samples, indicating excellent stability and integrity of our DNA walkers once synthesized for at least 3 weeks.

3.3. Feasibility test

We performed PAGE characterization to confirm the feasibility of our proposed method. Before we modified AuNPs with the thiolated substrate strand and caged enzyme strand, 12 % PAGE was employed to evaluate the feasibility of the sequence designs. As shown in Fig. 2A, a higher molecular weight band was detected in Lane 6 when we mixed the enzyme strand and locking strand compared with the molecular weights of the separate components in Lanes 2 and 3 respectively, indicating that the locking strand hybridized with the enzyme strand. In addition, the aforementioned hybridization complex was further mixed with the substrate strand (Lane 4) in Lane 8. A minimal change was observed in the band compared with Lane 6, except for the appearance of the substrate strand, suggesting that the enzyme strand was successfully caged by the locking strand and cannot hybridize with the substrate strand and, that the DNAzyme activity was inhibited as expected. As shown in Lane 7, when we mixed the hybridization complex present in Lane 6 with the DNA strand, the band intensity of the DNA strand decreased significantly compared with its corresponding band in Lane 5 (at the same concentrations). The enzyme band clearly reappeared, confirming that the locking strand hybridized with the DNA strand through toe-hold mediated strand displacement to free the enzyme strand as expected.

After confirming the successful design of the sequences and their behaviors in aqueous solution, we used the modified AuNPs to further evaluate the feasibility of the proposed method for detecting RNase H activity. As shown in Fig. 2B, DNA walker nanoprobes exhibited minimum fluorescence due to the quenching of FAM by AuNPs (blue curve). When we mixed the DNA walker probe with Mn^{2+} alone, there was no observable fluorescence recovery (black curve). Similarly, in the absence of Mn^{2+}, a minimal change in the fluorescence intensity was observed when the DNA walker probes were incubated with RNase H treated DNA/RNA complexes (green curve). However, when we mixed

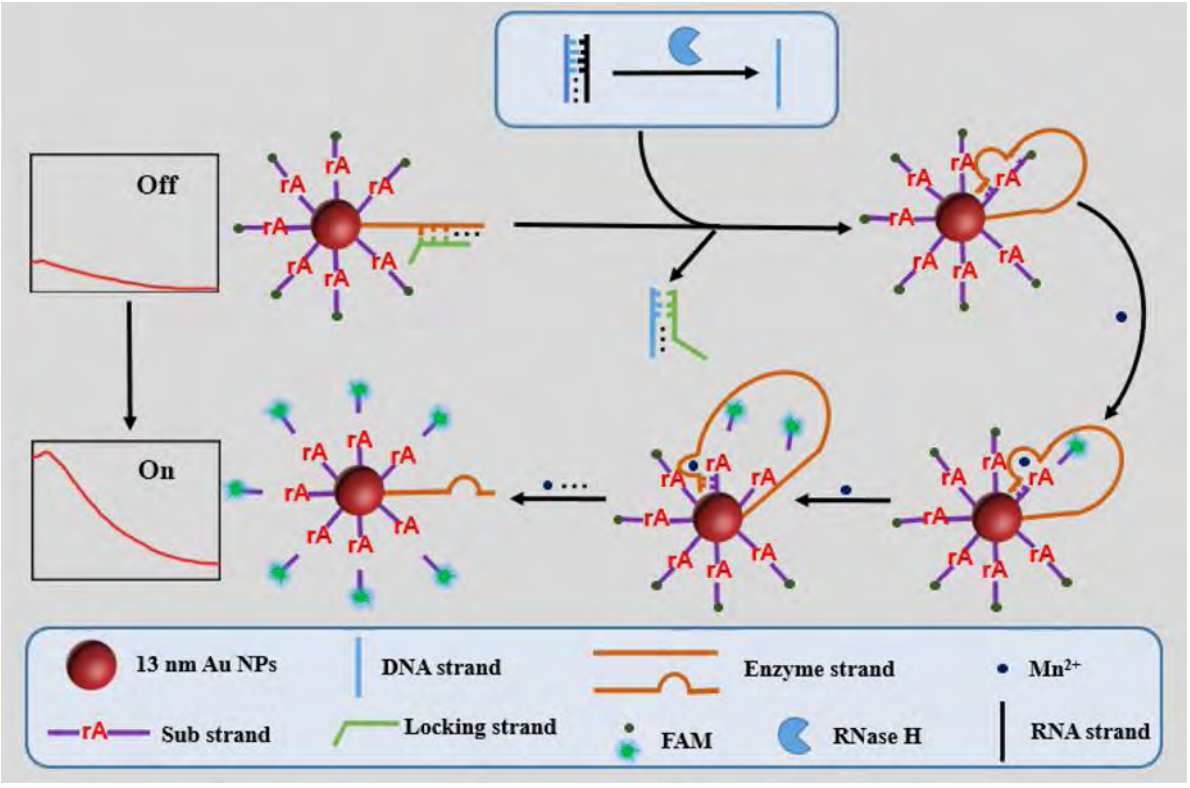

Scheme 1. Schematic diagram of RNase H activity detection using DNAzyme-powered on-particle DNA walker probes.

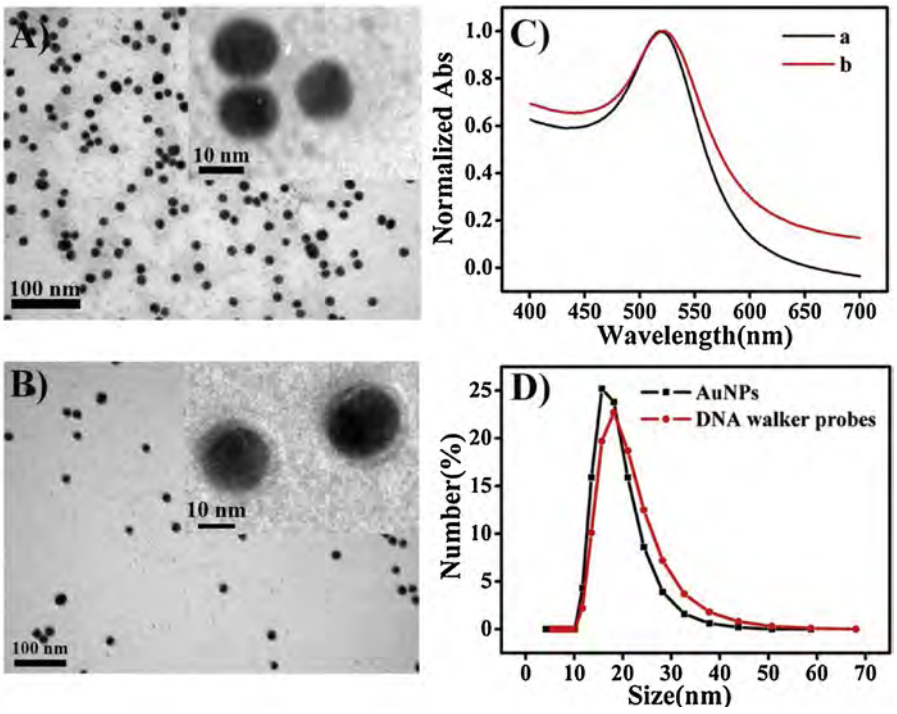

Fig. 1. Characterizations of probe. TEM images of A) AuNPs and B) DNA walker probes; C) UV–vis spectra of AuNPs (black curve) and DNA walker probes (red curve); D) Dynamic light scattering (DLS) of AuNPs (black curve) and DNA walker probes (red curve) (For interpretation of the references to colour in this figure legend, the reader is referred to the web version of this article.).

RNase H-treated DNA/RNA complexes with Mn^{2+} and DNA walker probes at the same time, a 3-fold increase in the fluorescence intensity was observed (red curve), indicating the feasibility of our proposed method for evaluating RNase H activity.

3.4. Optimization of experimental conditions

We first optimized the ratio of RNA and DNA in DNA/RNA complexes to achieve optimal biosensing performance. Before hydrolysis by RNase H, the DNA strand was not expected to be released to activate the DNAzyme-powered on-particle DNA walker; thus, the RNA to DNA ratio would be greater than 1. However, if the ratio was too high, the excess RNA would re-hybridize with the DNA to prevent the DNA strand from initiating the operation of the DNA walker. The ratio ranged from 1 to 2, as displayed in Fig. 3A, and the optimized ratio was 1.2:1. In addition, we also optimized the volume of the DNA walker

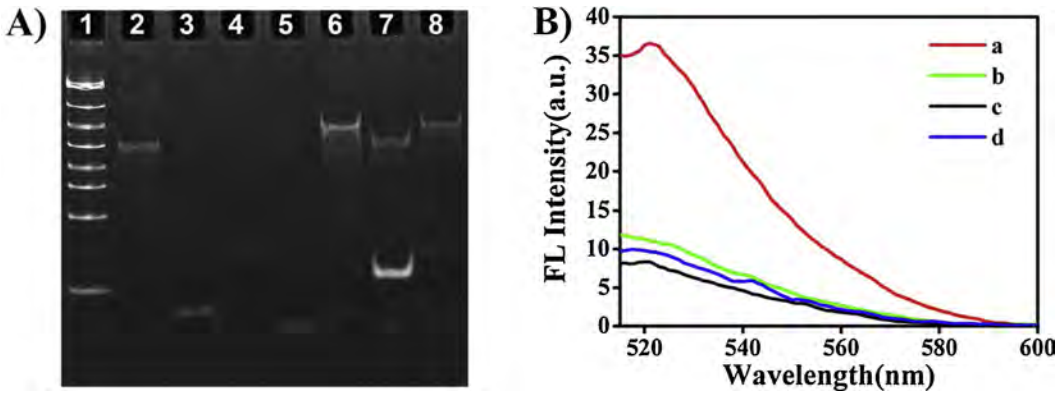

Fig. 2. Feasibility tests. A) 12% PAGE characterization. Lane 1: DNA marker; Lane 2: Enzyme strand; Lane 3: Locking strand; Lane 4: Substrate strand; Lane 5: DNA strand; Lane 6: Enzyme strand + Locking strand; Lane 7: Enzyme strand + Locking strand + DNA strand; Lane 8: Enzyme strand + Locking strand + Substrate strand. The concentration of all strands was 100 nM B) Fluorescence spectra for different samples. a: DNA walker probes + DNA/RNA + RNase H + Mn^{2+} (red curve); b: DNA walker probes + DNA/RNA + RNase H + EDTA (green curve); c: DNA walker probes + Mn^{2+} (black curve); d: DNA walker probes (blue curve). The excitation wavelength was 495 nm (For interpretation of the references to colour in this figure legend, the reader is referred to the web version of this article.).

probes. As shown in Fig. 3B, we varied the probe volumes from 0.1 μL to 1 μL. As the probe volume increased, the signal to background (S/B) ratio increased, exhibiting the highest S/B ratio at 0.5 μL. When the probe volume was less than 0.5 μL, the fluorescence signal was too low to achieve a low S/B ratio. However, when we used a volume greater than 0.5 μL, the background signal increased more than the recovery fluorescence signal, leading to a low S/B ratio; therefore, the probe volume was optimized to 0.5 μL.

3.5. Performance of the RNase H activity evaluation

Under the optimized conditions, we further evaluated the sensing performance of our proposed method. As shown in Fig. 4A, the fluorescence intensity increased in the presence of increasing concentrations of RNase H ranging from 0 U mL^{-1} to 5 U mL^{-1}. The relationship between the fluorescence intensity and RNase H concentration is shown in Fig. 4B. A good linear correlation was observed between the fluorescence intensity and logarithm of RNase H activity (inset in Fig. 4B). The regression equation was FL = 6.8 log C + 29 with a correlation coefficient of 0.9886. The limit of detection was calculated to be 0.00847 U mL^{-1} (S/N ≥ 3), which is comparable or superior to the previously reported methods shown in Table 1, revealing the excellent signal amplification of the on-particle DNA walker without a requirement for protein enzymes.

Several other enzymes, including Exo I, mung bean nuclease, Dpn I and Hind III, were employed under the same detection conditions with 5 times higher concentrations to confirm the selectivity of the proposed method for evaluating RNase H activity. As depicted in Fig. S6, a significant increase in the fluorescence intensity was only observed in the presence of RNase H. Meanwhile, the other enzymes caused negligible fluorescence increase compared with the blank sample lacking any enzyme, indicating the specific ability of RNase H to hydrolyze RNA in DNA/RNA chimeric complex. Based on this result, the method exhibited satisfactory selectivity in detecting RNase H activity.

3.6. Evaluation of RNase H inhibitor

A model inhibitor, ellipticine, was employed to assess the capability of our proposed method to screen RNase inhibitor, which is regarded to be promising candidate to combat intractable diseases such as AIDS. Ellipticine is a small molecule that is reported to preferentially target DNA/RNA hybrids, and the interaction of ellipticine with RNase H effectively inhibits enzymatic activity either by blocking enzyme binding or the interaction with the cleavage substrate [37]. As shown in Fig. 5, the fluorescence intensity decreased as the inhibitor concentration increased, verifying its ability to inhibit RNase H activity. Thus, the methodology described here is capable of screening inhibitors that block RNase H activity.

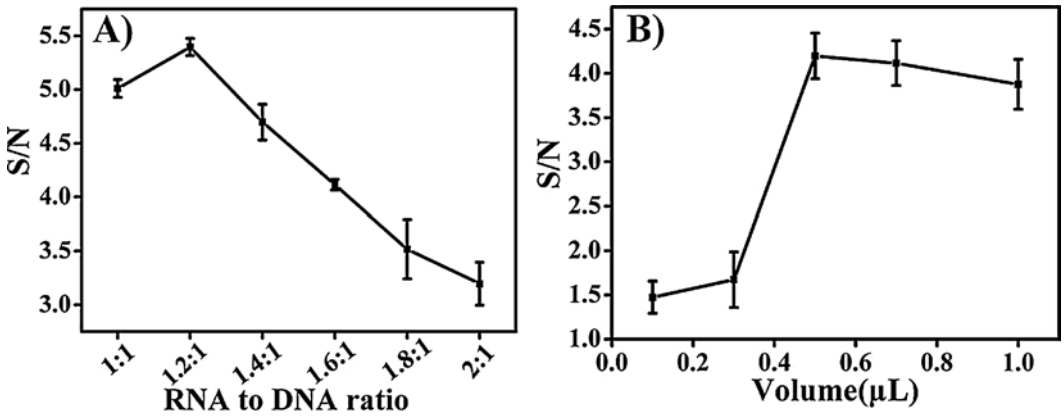

Fig. 3. Optimization of RNA/DNA Ratio (A) and Dosage of DNA walker probes.

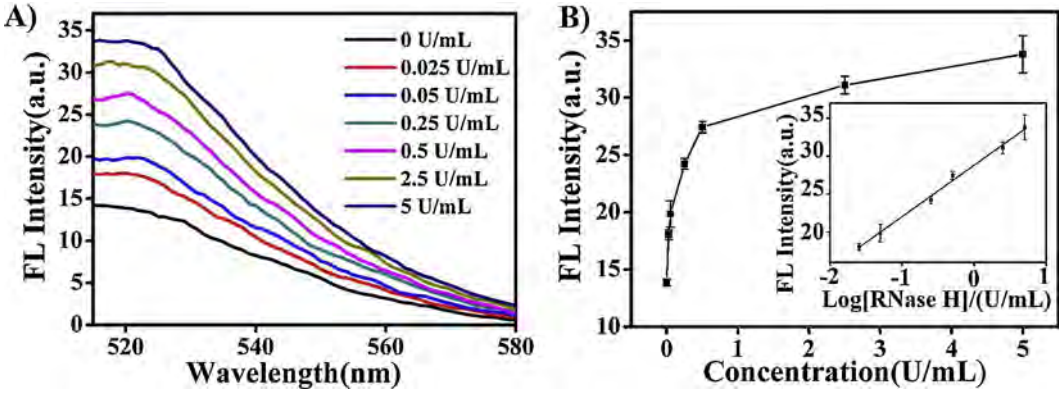

Fig. 4. Sensitivity of the RNase H activity assay. A) Fluorescence spectra of DNA walker probes with varied RNase H concentrations from 0 to 5 U/mL; B) Fluorescence intensities at 520 nm vs RNase H concentrations. Inset: logarithmic plot of fluorescence intensities vs RNase H at varying concentrations.

3.7. Evaluation of RNase H activity in cell lysates

We utilized cell lysates to verify the practicality of the proposed method for evaluating RNase H activity in a real sample. As illustrated in Fig. 6, F was the fluorescence intensity for different samples, and F_0 was the fluorescence intensity for DNA walker probes in buffer solution. The ratio F/F_0 was employed to evaluate the fluorescence recovery. When we mixed DNA walker probes with the HeLa cell lysate in the absence of RNase H and DNA/RNA complexes, minimal fluorescence recovery (a) was observed, verifying the excellent stability of the DNA walker probes for complex sample applications. Similarly, in the absence of RNase H, the mixture of DNA walker probes with Mn^{2+} and DNA/RNA complexes in a HeLa cell lysate showed negligible fluorescence recovery (b). Meanwhile, in the presence of RNase H, the simultaneous incubation of DNA/RNA complexes and Mn^{2+} with the HeLa cell lysate produced a 4 times fold increase in the fluorescence intensity (c), confirming the feasibility of the method for evaluating RNase H activity in a real sample. In addition to HeLa cell lysates, A549 cell lysates, HepG2 cell lysates and 4T1 cell lysates were also studied. When we added 5 U mL^{-1} RNase H in different cancer cell line lysates, nearly same fluorescence recovery signals were obtained (d, e and f), revealing the feasibility of our proposed method in various cell lysates.

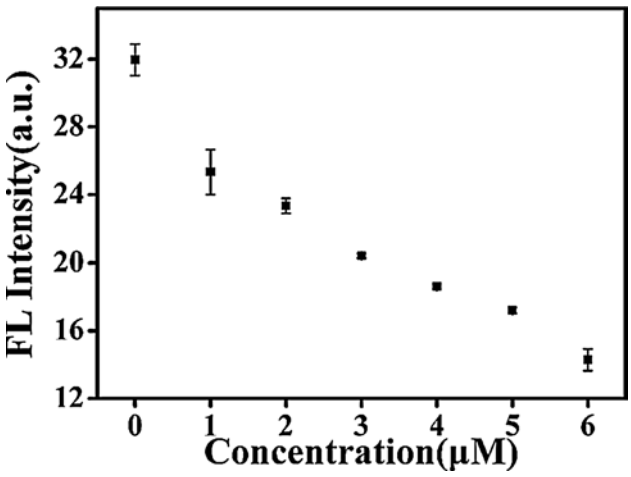

Fig. 5. Effect of increasing concentration of inhibitor ellipticine on RNase H activity. The fluorescence intensities at 520 nm under various concentrations was measured.

4. Conclusions

In conclusion, we have developed a sensitive method to evaluate the activity of RNase H using an on-particle DNA walker. The products generated by the RNase H-mediated hydrolysis of DNA/RNA complexes were able to active the DNAzyme walker to continuously cleave the labeled substrate strand, generating increased fluorescence to indicate the activity of RNase H. Taking advantage of the excellent signal amplification property of the DNAzyme-powered on particle DNA walker, a detection limit as low as 0.00847 U mL^{-1} was achieved. In addition, the method exhibited satisfactory selectivity for RNase H among several other enzymes. The proposed method can be implemented to screen RNase H inhibitors and facilitate drug development. The method also represents a promising tool to evaluate RNase H activity in real complex samples, such as cell lysates, for related biological studies.

Declaration of Competing Interest

The authors declare that they have no known competing financial interests or personal relationships that could have appeared to influence the work reported in this paper.

Table 1
Comparison of RNase H activity detection performance using different strategies.

Detection method	Dynamic range	LOD	Ref.
Fluorescent assay based on Mg^{2+} DNAzyme assisted cascade amplification	0.02-20 U mL^{-1}	0.01 U mL^{-1}	[16]
Fluorescent assay using iridium (III) complexes with 1,10-phenanthroline-based N^N ligands as highly selective luminescent G-quadruplex probes.	0.125-4 U mL^{-1}	0.125 U mL^{-1}	[19]
Fluorescent assay based on target-triggered catalytic haipin assembly signal amplification.	0-0.7 U mL^{-1}	0.037 U mL^{-1}	[20]
Fluorescent assay based on Tb^{3+}-induced G-quadruplex conjugates.	0-20 U mL^{-1}	2 U mL^{-1}	[21]
Fluorescent assay based on nicking enzyme assisted signal amplification.	0.03-1 U mL^{-1}	0.03 U mL^{-1}	[22]
Fluorescent assay based on DNAzyme-powered on-AuNPs DNA walker.	0-5 U mL^{-1}	0.00847 U mL^{-1}	This work

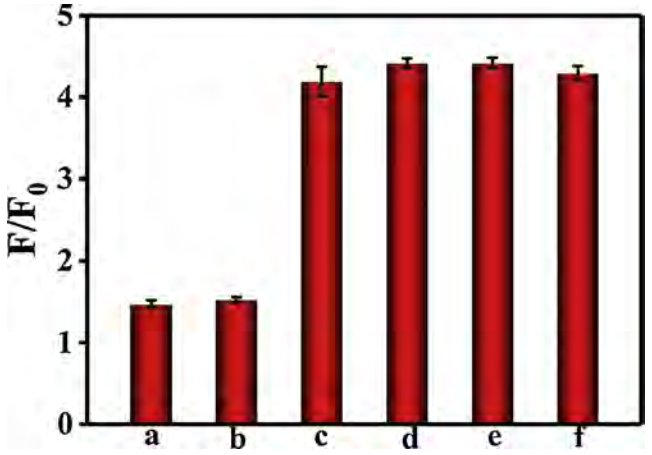

Fig. 6. Real sample fluorescence recovery for different samples. (a) DNA walker probes + HeLa cell lysate; (b) DNA walker probes + Mn^{2+} + DNA/ RNA + HeLa cell lysate; (c) DNA walker probes + Mn^{2+} + DNA/ RNA + HeLa cell lysate + RNase H; (d) DNA walker probes + Mn^{2+} + DNA/ RNA + A549 cell lysate + RNase H; (e) DNA walker probes + Mn^{2+} + DNA/ RNA + HepG2 cell lysate + RNase H; (f) DNA walker probes + Mn^{2+} + DNA/ RNA + 4T1 cell lysate + RNase H. The final concentration of RNase H is 5 U mL-.

Acknowledgements

This work was supported by National Natural Science Foundation of China (21804046, 21778020), Fundamental Research Funds for the Central Universities (2662018QD012), Natural Science Foundation of Hubei Province, China (2018CFB368) and Sci-tech Innovation Foundation of Huazhong Agriculture University (2662017PY042, 2662018PY024).

Appendix A. Supplementary data

Supplementary material related to this article can be found, in the online version, at doi:https://doi.org/10.1016/j.snb.2019.127380.

References

[1] H. Stein, P. Hausen, Enzyme from calf thymus degrading the RNA Moiety of DNA-RNA hybrids: effect on DNA-dependent RNA polymerase, Science 166 (1969) 393–395, https://doi.org/10.1126/science.166.3903.393.
[2] P. Hausen, H. Stein, Ribonuclease H: an enzyme degrading the RNA moiety of DNA-RNA hybrids, Eur. J. Biochem. 14 (1970) 278–283, https://doi.org/10.1111/j.1432-1033.1970.tb00287.x.
[3] W.F. Lima, S.T. Crooke, Binding affinity and specificity of escherichia coli RNase H1: impact on the kinetics of catalysis of antisense oligonucleotide − RNA hybrids, Biochemistry 36 (1997) 390–398, https://doi.org/10.1021/bi962230p.
[4] H. Nakamura, Y. Oda, S. Iwai, H. Inoue, E. Ohtsuka, S. Kanaya, S. Kimura, C. Katsuda, K. Katayanagi, K. Morikawa, How does RNase H recognize a DNA.RNA hybrid? Proc. Natl. Acad. Sci. 88 (1991) 11535–11539, https://doi.org/10.1073/pnas.88.24.11535.
[5] F. Lazzaro, D. Novarina, F. Amara, Danielle L. Watt, Jana E. Stone, V. Costanzo, Peter M. Burgers, Thomas A. Kunkel, P. Plevani, M. Muzi-Falconi, RNase H and postreplication repair protect cells from ribonucleotides incorporated in DNA, Mol. Cell 45 (2012) 99–110, https://doi.org/10.1016/j.molcel.2011.12.019.
[6] W.F. Lima, H.M. Murray, S.S. Damle, C.E. Hart, G. Hung, C.L. De Hoyos, X.-H. Liang, S.T. Crooke, Viable RNaseH1 knockout mice show RNaseH1 is essential for R loop processing, mitochondrial and liver function, Nucleic Acids Res. 44 (2016) 5299–5312, https://doi.org/10.1093/nar/gkw350.
[7] T. Ogawa, T. Okazaki, Function of RNase H in DNA replication revealed by RNase H defective mutants of Escherichia coli, Mol. Gen. Genet. 193 (1984) 231–237, https://doi.org/10.1007/BF00330673.
[8] M. Tisdale, T. Schulze, B.A. Larder, K. Moelling, Mutations within the RNase H domain of human immunodeficiency virus type 1 reverse transcriptase abolish virus infectivity, J. Gen. Virol. 72 (1991) 59–66, https://doi.org/10.1099/0022-1317-72-1-59.
[9] D.M. Himmel, N.S. Myshakina, T. Ilina, A. Van Ry, W.C. Ho, M.A. Parniak, E. Arnold, Structure of a dihydroxycoumarin active-site inhibitor in complex with the RNase H domain of HIV-1 reverse transcriptase and structure–activity analysis of inhibitor analogs, J. Mol. Biol. 426 (2014) 2617–2631, https://doi.org/10.1016/j.jmb.2014.05.006.
[10] P.L. Boyer, S.J. Smith, X.Z. Zhao, K. Das, K. Gruber, E. Arnold, T.R. Burke, S.H. Hughes, Developing and evaluating inhibitors against the RNase H active site of HIV-1 reverse transcriptase, J. Virol. 92 (2018) e02203–17, https://doi.org/10.1128/JVI.02203-17.
[11] D.M. Himmel, S.G. Sarafianos, S. Dharmasena, M.M. Hossain, K. McCoy-Simandle, T. Ilina, A.D. Clark, J.L. Knight, J.G. Julias, P.K. Clark, K. Krogh-Jespersen, R.M. Levy, S.H. Hughes, M.A. Parniak, E. Arnold, HIV-1 reverse transcriptase structure with RNase H inhibitor dihydroxy benzoyl naphthyl hydrazone bound at a novel site, ACS Chem. Bio. 1 (2006) 702–712, https://doi.org/10.1021/cb600303y.
[12] E. Kanaya, S. Kanaya, Kinetic analysis of escherichia coli ribonuclease HI using oligomeric DNA/RNA substrates suggests an alternative mechanism for the interaction between the enzyme and the substrate, Eur. J. Biochem. 231 (1995) 557–562, https://doi.org/10.1111/j.1432-1033.1995.0557d.x.
[13] K.C. Chan, S.R. Budihas, S.F.J. Le Grice, M.A. Parniak, R.J. Crouch, S.A. Gaidamakov, H.J. Isaaq, A. Wamiru, J.B. McMahon, J.A. Beutler, A capillary electrophoretic assay for ribonuclease H activity, Anal. Biochem. 331 (2004) 296–302, https://doi.org/10.1016/j.ab.2004.05.017.
[14] M.L. Dirksen, R.J. Crouch, Selective inhibition of RNase H by dextran, J. Bio. Chem. 256 (1981) 11569–11573, https://doi.org/10.1074/jbc.272.35.22023.
[15] Y. Zhang, Z. Li, Y. Cheng, X. Lv, Colorimetric detection of microRNA and RNase H activity in homogeneous solution with cationic polythiophene derivative, Chem. Commun. 45 (2009) 3172–3174, https://doi.org/10.1039/B904579A.
[16] L. Wang, H. Zhou, B. Liu, C. Zhao, J. Fan, W. Wang, C. Tong, Fluorescence assay for ribonuclease H based on nonlabeled substrate and DNAzyme assisted cascade amplification, Anal. Chem. 89 (2017) 11014–11020, https://doi.org/10.1021/acs.analchem.7b02899.
[17] S. Persano, G. Vecchio, P.P. Pompa, A hybrid chimeric system for versatile and ultra-sensitive RNase detection, Sci. Rep. 5 (2015) 1–5, https://doi.org/10.1038/srep09558.
[18] B. Liu, D. Xiang, Y. Long, C. Tong, Real time monitoring of junction ribonuclease activity of RNase H using chimeric molecular beacons, Analyst 138 (2013) 3238–3245, https://doi.org/10.1039/C3AN36414C.
[19] L. Lu, W. Wang, C. Yang, T.-S. Kang, C.-H. Leung, D.-L. Ma, Iridium(iii) complexes with 1,10-phenanthroline-based N^N ligands as highly selective luminescent G-quadruplex probes and application for switch-on ribonuclease H detection, J. Mater. Chem. B 4 (2016) 6791–6796, https://doi.org/10.1039/C6TB02316A.
[20] C.Y. Lee, H. Jang, K.S. Park, H.G. Park, A label-free and enzyme-free signal amplification strategy for a sensitive RNase H activity assay, Nanoscale 9 (2017) 16149–16153, https://doi.org/10.1039/C7NR04060A.
[21] K. Wu, C. Ma, H. Liu, H. He, W. Zeng, K. Wang, Label-free fluorescence assay for rapid detection of RNase H activity based on Tb3 + -induced G-quadruplex conjugates, Anal. Methods 9 (2017) 3055–3060, https://doi.org/10.1039/C7AY00709D.
[22] K. Wu, C. Ma, Z. Deng, N. Fang, Z. Tang, X. Zhu, K. Wang, Label-free and nicking enzyme-assisted fluorescence signal amplification for RNase H determination based on a G-quadruplexe/thioflavin T complex, Talanta 182 (2018) 142–147, https://doi.org/10.1016/j.talanta.2018.01.075.
[23] C. Zhao, J. Fan, L. Peng, L. Zhao, C. Tong, W. Wang, B. Liu, An end-point method based on graphene oxide for RNase H analysis and inhibitors screening, Biosens. Bioelectron. 90 (2017) 103–109, https://doi.org/10.1016/j.bios.2016.11.032.
[24] H. Zhang, M. Lai, A. Zuehlke, H. Peng, X.-F. Li, X.C. Le, Binding-induced DNA nanomachines triggered by proteins and nucleic acids, Angew. Chem. Int. Ed. Engl. 54 (2015) 14326–14330, https://doi.org/10.1002/anie.201506312.
[25] X. Yang, Y. Tang, S.D. Mason, J. Chen, F. Li, Enzyme-powered three-dimensional DNA nanomachine for DNA walking, payload release, and biosensing, ACS Nano 10 (2016) 2324–2330, https://doi.org/10.1021/acsnano.5b07102.
[26] Y. Li, G.A. Wang, S.D. Mason, X. Yang, Z. Yu, Y. Tang, F. Li, Simulation-guided engineering of an enzyme-powered three dimensional DNA nanomachine for discriminating single nucleotide variants, Chem. Sci. 9 (2018) 6434–6439, https://doi.org/10.1039/C8SC02761G.
[27] J. Chen, A. Zuehlke, B. Deng, H. Peng, X. Hou, H. Zhang, A target-triggered DNAzyme motor enabling homogeneous, amplified detection of proteins, Anal. Chem. 89 (2017) 12888–12895, https://doi.org/10.1021/acs.analchem.7b03529.
[28] H. Peng, X.-F. Li, H. Zhang, X.C. Le, A microRNA-initiated DNAzyme motor operating in living cells, Nat. Commun. 8 (2017) 14378–14380, https://doi.org/10.1038/ncomms14378.
[29] X. Qu, D. Zhu, G. Yao, S. Su, J. Chao, H. Liu, X. Zuo, L. Wang, J. Shi, L. Wang, W. Huang, H. Pei, C. Fan, An exonuclease III-powered, on-particle stochastic DNA walker, Angew. Chem. Int. Ed. Engl. 56 (2017) 1855–1858, https://doi.org/10.1002/anie.201611777.
[30] C.-P. Liang, P.-Q. Ma, H. Liu, X. Guo, B.-C. Yin, B.-C. Ye, Rational engineering of a dynamic, entropy-driven DNA nanomachine for intracellular MicroRNA imaging, Angew. Chem. Int. Ed. Engl. 56 (2017) 9077–9081, https://doi.org/10.1002/anie.201704147.
[31] P.-Q. Ma, C.-P. Liang, H.-H. Zhang, B.-C. Yin, B.-C. Ye, A highly integrated DNA nanomachine operating in living cells powered by an endogenous stimulus, Chem. Sci. 9 (2018) 3299–3304, https://doi.org/10.1039/C8SC00049B.
[32] L. Zhu, Q. Liu, B. Yang, H. Ju, J. Lei, Pixel counting of fluorescence spots triggered

by DNA walkers for ultrasensitive quantification of nucleic acid, Anal. Chem. 90 (2018) 6357–6361, https://doi.org/10.1021/acs.analchem.8b01146.
[33] X. Yang, D. Shi, S. Zhu, B. Wang, X. Zhang, G. Wang, Portable aptasensor of aflatoxin B1 in bread based on a personal glucose meter and DNA walking machine, ACS Sens. 3 (2018) 1368–1375, https://doi.org/10.1021/acssensors.8b00304.
[34] J. Liu, Y. Lu, Preparation of aptamer-linked gold nanoparticle purple aggregates for colorimetric sensing of analytes, Nat. Protoc. 1 (2006) 246–252, https://doi.org/10.1038/nprot.2006.38.
[35] Q. Mei, X. Wei, F. Su, Y. Liu, C. Youngbull, R. Johnson, S. Lindsay, H. Yan, D. Meldrum, Stability of DNA origami nanoarrays in cell lysate, Nano Lett. 11 (2011) 1477–1482, https://doi.org/10.1021/nl1040836.
[36] L. Wu, G. Li, X. Xu, L. Zhu, R. Huang, X. Chen, Application of nano-ELISA in food analysis: recent advances and challenges, TrAC Trends in Anal. Chem. 113 (2019) 140–156, https://doi.org/10.1016/j.trac.2019.02.002.
[37] J. Ren, X. Qu, N. Dattagupta, J.B. Chaires, Molecular recognition of a RNA:DNA hybrid structure, J. Am. Chem. Soc. 123 (2001) 6742–6743, https://doi.org/10.1021/ja015649y.

Wenjing Wang is currently an associate professor in the College of Science of Huazhong Agricultural University. She received her PhD degree from Nanjing University in 2017. Her research interests include biochemical analysis, DNA nanotechnology-based biosensing and bioimaging.

Mingbo Shu is a graduate student major in chemistry.

Axiu Nie is a graduate student major in chemistry.

Heyou Han received his PhD in analytical chemistry from the Wuhan University in 2000. From 2000 to 2002, he was a postdoctoral researcher at the University of Science and Technology of China. Currently, He is a professor in the State Key Laboratory of Agricultural Microbiology, College of Science from Huazhong Agricultural University (China). He also served as the Executive Vice Dean of the Graduate School in Huazhong Agricultural University. His research mainly focuses on developing new analysis methods to detect pathogenic microorganisms including virus and bacteria in agriculture.